Journal of Power Sources 232 (2013) 93–98

Contents lists available at SciVerse ScienceDirect

Journal of Power Sources

journal homepage: www.elsevier.com/locate/jpowsour

Short communication

A current-sensor electrochemical device for accurate gas diffusivity measurement in fuel cells

Weidong He [a,b,*], Bin Wang [c]

[a] Interdisciplinary Program in Materials Science, Vanderbilt University, Nashville, TN 37235, USA
[b] Vanderbilt Institute of Nanoscale Science and Engineering, Vanderbilt University, Nashville, TN 37235, USA
[c] Department of Physics and Astronomy, Vanderbilt University, Nashville, TN 37235, USA

HIGHLIGHTS

- Designs a current-sensor device for accurate fuel cell diffusivity measurement.
- Improves evaluation accuracy of concentration polarization & limiting current.
- Shows that the proposed device is reliable for fuel cell electrode pre-evaluation.

GRAPHICAL ABSTRACT

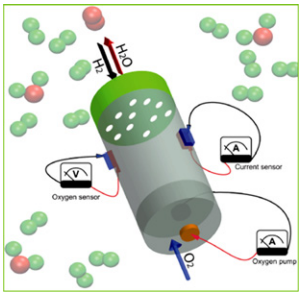

ARTICLE INFO

Article history:
Received 21 August 2012
Received in revised form
4 January 2013
Accepted 5 January 2013
Available online 16 January 2013

Keywords:
Fuel cells
Diffusivities
Limiting current densities
Electrode thicknesses
Oxygen sensors
Concentration polarizations

ABSTRACT

In the previous diffusivity measurements via the electrochemical devices designed by the authors, the electronic conduction contribution of electrolyte materials was neglected, and an error in the subsequent evaluations of limiting current density and concentration polarization was consequently induced. In this report, a current-sensor and oxygen-sensor based electrochemical cell was designed for accurate diffusivity measurements in fuel cells. Our analytical investigation shows that diffusivity measurements via the new device lead to accurate analytical evaluations of limiting current density and concentration polarization in fuel cells. With the improved accuracy, one can reliably pre-evaluate the limiting current density and concentration polarization of fuel cell electrodes with different thicknesses ranging from several nanometers to a few millimeters at different operating temperatures.

Published by Elsevier B.V.

1. Introduction

To facilitate the sustainable advancement of our society, reducing energy crisis has become more urgent than ever. Hydrogen-based fuel cells have emerged into an efficient component in current renewable energy policy. Many novel materials and structures have been developed to improve the energy conversion efficiency and lifetime of the existing fuel cell devices, including solid oxide fuel cells (SOFCs), proton exchange membrane fuel cells (PEMFCs), and molten carbonate fuel cells (MCFCs) [1–5]. In particular, highly-porous nanostructured electrodes have drawn tremendous research interest in the past decade due to their promising features, such as pronounced mechanical strength, and low polarization loss [6–9]. Among the polarization losses of fuel cells, including concentration polarization (*CP*), Ohmic loss (*OL*) and activation loss (*AL*), *CP* is a function of gas diffusivity in fuel cells,

* Corresponding author. Interdisciplinary Program in Materials Science, Vanderbilt University, Nashville, TN 37235, USA. Tel.: +1 6153647338; fax: +1 6153437263.
E-mail address: weidong.he@vanderbilt.edu (W. He).

0378-7753/$ – see front matter Published by Elsevier B.V.
http://dx.doi.org/10.1016/j.jpowsour.2013.01.032

and reliable gas diffusivity measurements can help one to make efficient strategies to reduce the *CP* of a fuel cell system [10–13]. *CP* is a function of gas diffusivity, which correlates with the important parameters associated with an electrode, such as porosity and tortuosity, as shown in Eqs. (1)–(4),

$$\eta_a = -\frac{RT}{2F}\ln\left(1-\frac{i}{i_a}\right) + \frac{RT}{2F}\ln\left(1+\frac{p^{\circ}_{H_2} i}{p^{\circ}_{H_2O} i_a}\right) \quad (1)$$

$$\eta_c = -\frac{RT}{4F}\ln\left(1-\frac{i}{i_c}\right) \quad (2)$$

$$D^{\text{eff}}_{H_2-H_2O} = \frac{\varphi_q}{\tau_a} D_{H_2-H_2O} \quad (3)$$

$$D^{\text{eff}}_{O_2-N_2} = \frac{\varphi_c}{\tau_c} D_{O_2-N_2} \quad (4)$$

where $\eta_a(\eta_c)$ is the anode (cathode) concentration polarization, $p^o_{H_2}(p^o_{H_2O})$ is the pressure of anode H_2 (H_2O) gas, i is the operating current, $i_a(i_c)$ is the diffusivity-dependent anode (cathode) limiting current density (*LCD*), F is the Faraday constant, R is the gas constant, T is the operating temperature, $D^{\text{eff}}_{H_2-H_2O}(D^{\text{eff}}_{O_2-N_2})$ is the effective binary anode (cathode) gas diffusivity, $\tau_a(\tau_c)$ is the anode (cathode) tortuosity factor, $\varphi_a(\varphi_c)$ is the volumetric porosity of the anode (cathode), and $D_{H_2-H_2O}(D_{O_2-N_2})$ is the bulk binary anode (cathode) diffusivity defined by Chapman–Enskog relation [13–15]. Unlike the measurement techniques of ionic conduction, such as electrochemical impedance spectroscopy, and nuclear magnetic resonance spectroscopy, which have been developed since decades ago, a traditional evaluation of gas diffusivity is typically done through mathematical fittings on the data of multiple voltage–current measurements on intact fuel cells [16–19]. Techniques of directly measuring effective binary gas diffusivities of electrodes in fuel cells in an out-of-cell fashion have only been developed in recent years [20–23]. Although the electrochemical devices allowed one to measure the gas diffusivity and evaluate the polarization loss as well as limiting current density in fuel cells, the accuracy of the measurement is still in debate; the measurement is based on the assumption that little electronic conduction through the electrolyte disc contributes to the current provided through the oxygen pump [21]. In the actual operation of an SOFC system, both ionic and electronic conductions can contribute to the electrical conduction of an electrolyte and thus, ignoring electronic contribution can cause inaccuracy in the gas diffusivity measurement and in the subsequent evaluation of limiting current density and concentration polarization loss [1].

In this Communication, an electrochemical cell with a current meter that reads the current only induced by ionic conduction, is proposed and analyzed. The correlation between the measurement uncertainty of the applied current and the evaluation errors of different parameters, such as diffusivity *CP*, and *LCD*, is investigated. The analysis shows that the proposed electrochemical device is highly favorable for accurate gas diffusivity measurements in fuel cells. The accurate diffusivity measurements lead to the accurate evaluation of concentration polarization loss and limiting current density in fuel cells, which is practically significant for the reliable and efficient pre-evaluation of electrodes before their assembly in intact fuel cells.

2. Materials and methods

2.1. Current-sensor based electrochemical cell device

The device can be employed to measure the gas diffusivity in any type of fuel cells, and for each type of fuel cells, specific electrolyte and electrode materials should be selected to measure the gas diffusivity in the operating conductions of fuel cells. Fig. 1 shows a schematic of the proposed electrochemical device for anode gas diffusivity measurements in solid oxide fuel cells. A yttria-stablized-zirconia (YSZ) tube is employed to create an isolated electrochemical cell system. A YSZ disc is attached to one end of the YSZ tube, and an anode sample to be measured is attached to the other end of the tube. A current provider is attached across the YSZ disc to be employed as an oxygen pump, and a voltage meter is attached to the YSZ tube to be used as an oxygen sensor. Previously, the applied current provided by the oxygen pump, the current measured with the oxygen sensor, and the equilibrium equation for H_2O, H_2 and O_2 phases were combined to measure the effective binary diffusivity of H_2 in porous anodes [20,21]. The electrical conduction in a ceramic fuel cell electrolyte can be contributed by both electronic and ionic species and thus, the applied current provided the oxygen pump is caused by the electronic and ionic conduction in the YSZ electrolyte [1,16]. This can introduce an inaccuracy in the subsequent calculation of effective binary diffusivities in fuel cells. Therefore, we need to improve the devices such that the ionic current induced by O^{2-} ions can be accurately measured. Differently from the reported gas diffusivity measurement devices, in this report a current meter is attached across the YSZ tube to measure the current only induced by O^{2-} conduction during the gas diffusivity measurement, as shown in Fig. 1.

2.2. Theoretical analysis

In anode diffusivity measurements, a H_2/H_2O gas mixture can be used. Upon the supply of a current via the oxygen pump, H_2/H_2O fluxes will be induced through the anode sample, according to Eq. (5),

$$J_{H_2} = -J_{H_2O} = \frac{i}{4F} \quad (5)$$

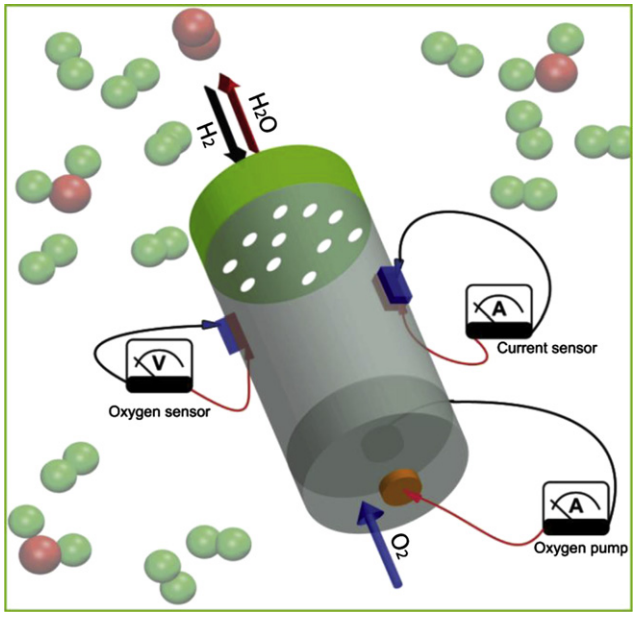

Fig. 1. A modified electrochemical device with a current sensor for accurate gas diffusivity measurement in solid oxide fuel cells. The device is placed inside a sealed tube furnace, H_2/H_2O or O_2/N_2 gas is driven into the tube furnace with a certain flow rate, and the system is then heated to the temperature at which diffusivity measurement is conducted. The directions of H_2/H_2O fluxes induced by the current provided via the oxygen pump, are demarcated by black/red arrows. (For interpretation of the references to color in this figure legend, the reader is referred to the web version of this article.)

where J_{H_2} (J_{H_2O}) is the H_2 (H_2O) flux induced by the applied current i. Due to the O_2 pressure difference between inside and outside of the YSZ tube, the voltage meter will read a voltage. Since O^{2-} diffuses through the YSZ tube, an electrical flow will be formed across the current meter and thus, the current meter will read a current. The measured current is induced by the O_2 pressure difference, and only corresponds to the ionic conduction of O^{2-} in the YSZ material. Therefore, in Eq. (5), the current value measured via the current meter, instead of the current provided via the oxygen pump, should be used to calculate the gas diffusivity. Such an adjustment is necessary especially as a substantial portion of the current provided via the O_2 pump is contributed by electronic conduction in the electrolyte disc. The evaluation of the adjustment should be based on quantitative analysis of the correlation between the uncertainty of the current measurement via previous devices and the evaluation errors of gas diffusivity, limiting current density, and concentration polarization. To present a conclusive quantitative analysis on the evaluation errors induced by the current uncertainty, in this report we allow current uncertainty to vary within (100% although electronic conduction typically results in a small percent of contribution to the total electrical conduction in the electrolyte materials of fuel cells [1,24–26].

3. Results and discussion

The evaluation error of effective binary H_2/H_2O (O_2/N_2) diffusivity induced by current measurement uncertainty is expressed in Eqs. (6) and (7),

$$\Delta D^{\text{eff}}_{H_2-H_2O} = \frac{RTl_a}{4F\left(p^o_{H_2} - p^i_{H_2}\right)}\Delta i \tag{6}$$

$$\Delta D^{\text{eff}}_{O_2-N_2} = \frac{RTl_c}{8F\left(p^i_{O_2} - p^o_{O_2}\right)}\Delta i \tag{7}$$

where $p^i_{H_2}$ ($p^i_{O_2}$) is the H_2 (O_2) pressure in the YSZ tube, and $p^o_{O_2}$ is the pressure of cathode gas. $p^i_{H_2}$ can be obtained via the voltage measurement using the oxygen sensor and with the reaction equilibrium constant of $H_2O/H_2/O_2$ system at a specific temperature [21]. ΔD is linearly dependent on Δi as a certain current is provided via the oxygen pump, as shown in Eqs. (6) and (7). With $p^i_{H_2}$ set as a temperature-dependent parameter, $\Delta D - \text{versus} - \Delta i/i$ dependences at different temperatures can be readily plotted. As shown in Fig. 2, for both anode (Fig. 2a) and cathode (Fig. 2b), $\Delta D - \text{versus} - \Delta i/i$ plots show obvious slopes; a 10% percent uncertainty of current measurement induces a 0.006 $cm^2\ s^{-1}$ (0.007 $cm^2\ s^{-1}$) error in anode (cathode) gas diffusivity measurement at 700 °C, indicating that the accuracy of anode/cathode diffusivity measurement is highly sensitive to the uncertainty of current measurement. One can notice that, with fixed current uncertainty, ΔD increases with increasing temperature for both anodes and cathodes. This suggests that high-temperature electrode diffusivity measurement should be done with the modified device instead of the previous electrochemical devices; such an adjustment appears to be less necessary for low-temperature SOFCs, which have long been favored and have remained to be the major research focus in the SOFC field.

Limiting current density is an important parameter for energy conversion systems, and correlates with the current utilization and the polarization loss of fuel cells [22,23,27–30]. Efficient diffusivity measurement directly leads to the evaluation on the limiting current densities of a fuel cell system. Anode limiting current density i_a and cathode limiting current density i_c exhibit linear dependence on diffusivity and thus, $\Delta i_a(\Delta i_c)$ also shows a linear dependence on Δi, as shown in Eqs. (8) and (9),

$$\Delta i_a \approx \frac{4Fp^o_{H_2}\Delta D^{\text{eff}}_{H_2-H_2O}}{RTl_a} \tag{8}$$

$$\Delta i_c \approx \frac{8Fp^o_{H_2}\Delta D^{\text{eff}}_{O_2-N_2}}{RTl_c}\left(\frac{p_t}{p_t - p^o_{O_2}}\right) \tag{9}$$

where p_t (~1 atm) is the total gas pressure in the measurement system. Based on Eqs. (8) and (9), $\Delta i_a(\Delta i_c)$ can be plotted as a function of Δi. As shown in Fig. 3, similar to the $\Delta D^{\text{eff}}_{H_2-H_2O}(\Delta D^{\text{eff}}_{O_2-N_2}) - \text{versus} - \Delta i/i$ plots, $\Delta i_a(\Delta i_c)$-versus-$\Delta i/i$ plots also show notable slopes; for anodes, the slope for 800 °C is 1646.3 A m^{-2}, followed by 1505.2 A m^{-2} for 750 °C, 1478.3 A m^{-2} for 700 °C, and 1331.5 A m^{-2} for 650 °C, respectively. Compared with the $\Delta D - \text{versus} - \Delta i/i$ plots, $\Delta i_a(\Delta i_c)$ shows a weaker temperature dependence. For instance, Δi_c does not show obvious temperature dependence, as confirmed by the similar slopes that the Δi_c-versus-$\Delta i/i$ plots at different temperatures have; the slope of the Δi_c-versus-$\Delta i/i$ plot only varies by 4.4% as the operating temperature changes from 650 °C to 800 °C. Comparing anodes and cathodes, while Δi_a-versus-$\Delta i/i$ plots at different temperatures are still distinguishable, the Δi_c-versus-$\Delta i/i$ plots at different temperatures almost overlap. This implies that lowering operating temperature cannot effectively reduce the cathode limiting current

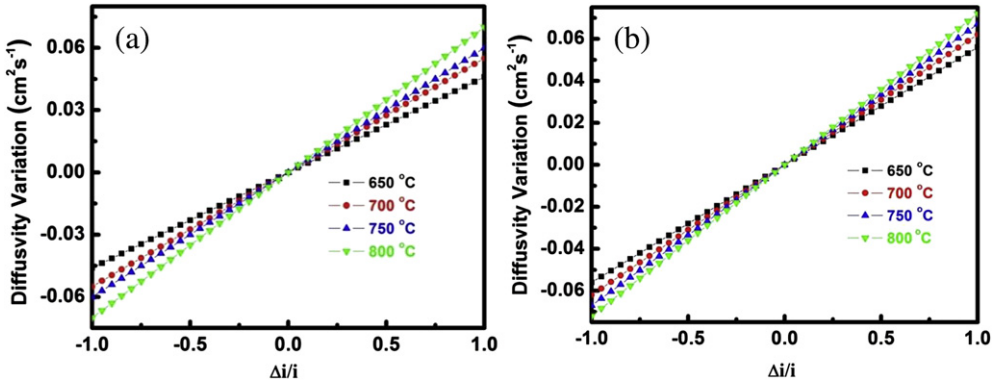

Fig. 2. Anode (a) and cathode (b) diffusivity measurement errors as a function of current measurement uncertainty ($\Delta i/i$) induced by ignoring electronic conduction contribution of electrolyte with an applied current density of 500 A m^{-2}. Anode thickness is 0.75 mm, and cathode thickness is 0.2 mm. Anode hydrogen effective binary diffusivities are 0.07 $cm^2\ s^{-1}$ for 800 °C, 0.06 $cm^2\ s^{-1}$ for 750 °C, 0.055 $cm^2\ s^{-1}$ for 700 °C, and 0.046 $cm^2\ s^{-1}$ for 650 °C, respectively. Cathode oxygen effective binary diffusivities are 0.072 $cm^2\ s^{-1}$ for 800 °C, 0.067 $cm^2\ s^{-1}$ for 750 °C, 0.062 $cm^2\ s^{-1}$ for 700 °C, and 0.056 $cm^2\ s^{-1}$ for 650 °C, respectively.

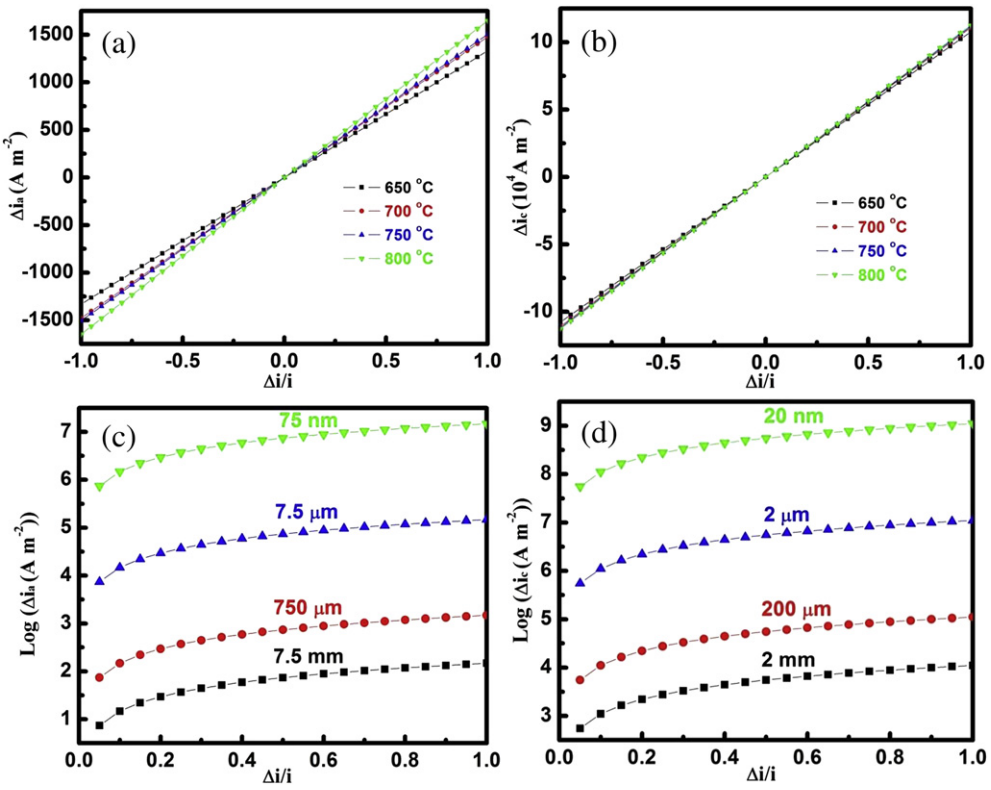

Fig. 3. Anode (a) and cathode (b) limiting current density evaluation errors as a function of current measurement uncertainty ($\Delta i/i$) induced by ignoring electronic conduction contribution of electrolyte with an applied current density of 500 A m^{-2}. Anode thickness is 0.75 mm, and cathode thickness is 0.2 mm. Anode limiting current densities are 1.65×10^3 A m^{-2} for 800 °C, 1.51×10^3 A m^{-2} for 750 °C, 1.48×10^3 A m^{-2} for 700 °C, and 1.33×10^3 A m^{-2} for 650 °C, respectively. Cathode limiting current densities are 11.25×10^4 A m^{-2} for 800 °C, 11.17×10^4 A m^{-2} for 750 °C, 11.07×10^4 A m^{-2} for 700 °C, and 10.77×10^4 A m^{-2} for 650 °C, respectively. Log(Δi_a)(Log(Δi_c))-versus-$\Delta i/i$ plots for different anode (c) (cathode (d)) thicknesses with an operating temperature of 700 °C and an applied current density of 500 A m^{-2}.

density measurement error induced by the current uncertainty in the cathode gas diffusivity measurement. Therefore, the improved electrochemical device shown in Fig. 1 is more necessary for the accurate evaluation of cathode limiting current density compared to the evaluation of anode limiting current density.

To improve the electrochemical performance and mechanical strength of fuel cells, nanostructured electrodes and electrolytes have been proposed and investigated [1,6–9,31–36]. In particular, thin electrodes have been proven to own many advantages over bulk electrodes, such as high gas diffusion rate, larger limiting current density, and low polarization loss, among others [6–8]. Previously-designed electrochemical devices were shown to have promising potential for the application of efficient gas diffusivity measurement and polarization loss evaluation in nanostructured fuel cells [21–23]. Therefore, an analytical evaluation on the diffusivity measurement error in nanostructured fuel cells using previously-proposed electrochemical devices is of practical significance. Fig. 3c and d show Log(Δi_a)(Log(Δi_c)) – versus – $\Delta i/i$ plots for the anode (cathode) of a fuel cell. With a fixed current measurement uncertainty, the plots for the four different electrode thicknesses follow similar trends, and the evaluation error of limiting current density increases with reducing the anode (cathode) thickness; with the same Δi, Log(Δi_a)(Log(Δi_c)) for 75 nm anode (20 nm cathode) is the largest among the four thicknesses, followed by those for 7.5 μm anode (2 μm cathode), 750 μm anode (200 μm cathode), and 7.5 mm anode (2 mm cathode), respectively. This means that the aforementioned modification of the gas diffusivity measurement devices is more necessary for limiting current density evaluation on thin nanostructured electrodes compared to bulk electrodes. Therefore, the device modification as proposed in this report is highly favorable as new nanostructured fuel cell electrodes are developed and are subject to pre-evaluation.

The key goal of employing the previously-reported oxygen-sensor based electrochemical devices is to pre-evaluate the polarization loss of fuel cell systems in an out-of-cell fashion through the direct gas diffusivity measurement [22]. The reliability of the gas diffusivity measurement directly impacts the accuracy of the polarization loss pre-evaluation. The correlation between the evaluation error of anode (cathode) concentration polarization loss and the current measurement uncertainty is described in Eqs. (10) and (11),

$$\Delta\eta_a = -\frac{RT}{2F}\ln\left(1-\frac{\Delta i}{i_a}\right) + \frac{RT}{2F}\ln\left(1+\frac{p^o_{H_2}\Delta i}{p^o_{H_2O} i_a}\right) \quad (10)$$

$$\Delta\eta_c = -\frac{RT}{4F}\ln\left(1-\frac{\Delta i}{i_c}\right) \quad (11)$$

where $\Delta\eta_a(\Delta\eta_c)$ is the anode (cathode) concentration polarization evaluation error induced by current value uncertainty in the anode (cathode) gas diffusivity measurement via previous electrochemical devices. Fig. 4a and Fig. 4b show the ΔCP – versus – $\Delta i/i$ plots for anodes and cathodes at different temperatures. The plots for cathodes resemble the $\Delta i_a(\Delta i_c)$ – versus – $\Delta i/i$ plots, but differently from the $\Delta i_a(\Delta i_c)$ – versus – $\Delta i/i$ plots, for the four temperatures, the slopes of ΔCP – versus – $\Delta i/i$ plots for anodes all increase with increasing Δi from −1 to 1. This indicates that an increased electronic conduction contribution can indeed result in increased sensitivity of polarization loss evaluation error resulted from current measurement uncertainty, and thus, the reliability of

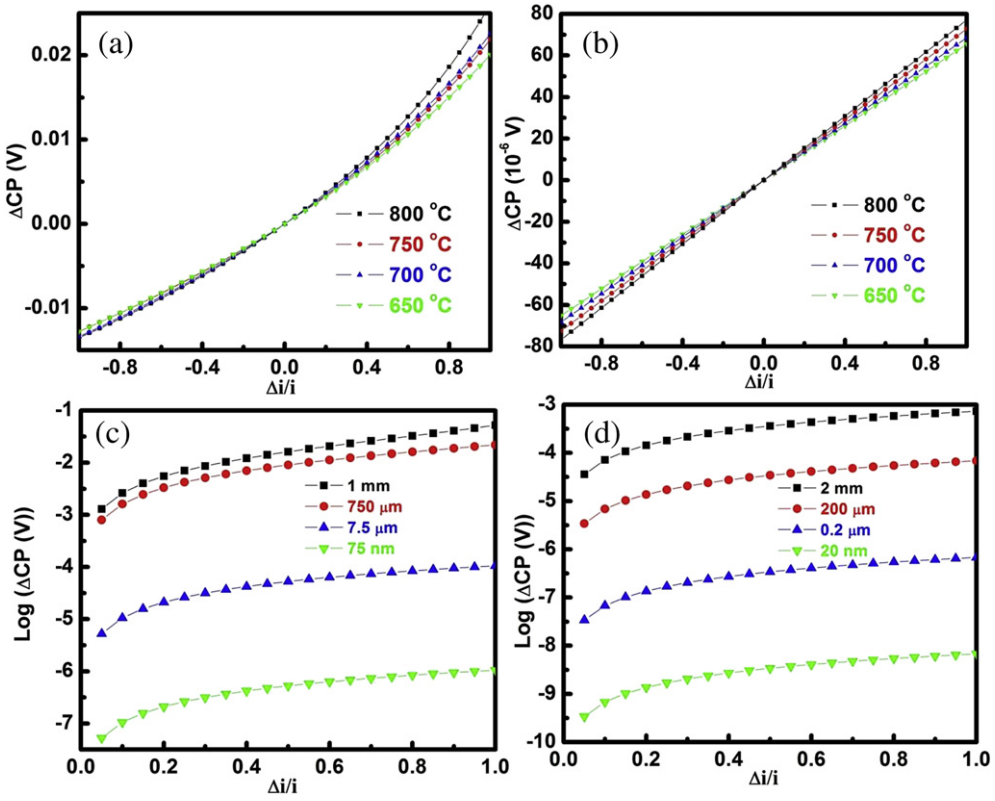

Fig. 4. Anode (a) and cathode (b) concentration polarization evaluation errors as a function of current measurement uncertainty ($\Delta i/i$) induced by ignoring electronic conduction contribution of electrolyte. Anode thickness is 0.75 mm, and cathode thickness is 0.2 mm. Anode concentration polarizations are 0.0135 V for 800 °C, 0.0128 V for 750 °C, 0.0134 V for 700 °C, and 0.0128 V for 650 °C, respectively. Cathode concentration polarizations are 7.7×10^{-4} V for 800 °C, 7.2×10^{-4} V for 750 °C, 6.8×10^{-4} V for 700 °C, and 6.5×10^{-4} V for 650 °C, respectively. Log(ΔCP) – versus – $\Delta i/i$ plots for different anode (c) cathode (d) thicknesses with an operating temperature of 700 °C and an applied current density of 500 A m^{-2}.

the previously-reported electrochemical devices decreases as the electronic contribution of the electrolyte tube and dics components increases. One can also notice that the increasing trend of this sensitivity with respect to Δi, appears to be more obvious at higher gas diffusivity measurement temperatures, as confirmed by the spead-out feature of the anode ΔCP – versus – $\Delta i/i$ plots at 650 °C, 700 °C, 750 °C, and 800 °C. With the same Δi, the anode ΔCP at 700 °C appears to be larger than the anode ΔCP at 750 °C, which is somewhat similar to the crossing features observed in the previous *CP* evaluations [22,23].

Fig. 4c and d show that the Log(ΔCP) – versus – $\Delta i/i$ plots for different anode (cathode) thicknesses at 700 °C. For each anode (cathode) thickness, the Log(ΔCP) – versus – $\Delta i/i$ plot looks similar to the Log(Δi_a)(Log(Δi_c)) – versus – $\Delta i/i$ plots. However, the thickness dependence of Log(ΔCP) – versus – $\Delta i/i$ plots appears to be opposite to the thickness dependence of the Log(Δi_a)(Log(Δi_c)) – versus – $\Delta i/i$ plots; Log(ΔCP) increases with increasing the electrode thickness whereas Log(Δi_a)(Log(Δi_c)) decreases with increasing electrode thickness. Cathode ΔCP exhibits a higher thickness dependence than anode ΔCP does. For example, ΔCP reaches an infinite value as the cathode thickness exceeds 1.0 mm while anode Log(ΔCP) – versus – $\Delta i/i$ dependence is still plottable with an anode thickness above 7.5 mm. The opposite dependence, as shown here, suggests that for thin electrodes, the accuracy of polarization loss evaluation is less sensitive to the current measurement uncertainty compared with thick electrodes. Therefore, compared with thin electrodes, an accurate polarization loss evaluation on thick electrodes tolerates less electronic contribution of electrolytes. The opposite dependences of Log(Δi_a)(Log(Δi_c)) – versus – $\Delta i/i$ plots and Log(ΔCP) – versus – $\Delta i/i$ plots suggest that the evaluation errors of $\Delta i_a(\Delta i_c)$ and ΔCP cannot be both reduced by reducing or increasing the electrode thickness; the accurate evaluation of both parameters should be based on the diffusivity measurement via the modified device as shown in Fig. 1.

Recently, the authors proposed the use of double-sensor and multi-sensor electrochemical devices for efficient gas diffusivity measurements in fuel cells [21,22]. Here, we propose that the improvement as analyzed in this report should be applied to all the devices for accurate gas diffusivity measurement in all types of fuel cells. The correlation between the evaluation errors of limiting current density and polarization loss with other parameters of fuel cell electrodes, such as porosity, tortuosity, and Knudsen number, will be the focus of future research.

In summary, a current sensor has been proposed to be added in the electrochemical devices for accurate anode/cathode diffusivity measurement in fuel cells. The analysis on the evaluation errors of diffusivity, limiting current density, and concentration polarization verifies that the improvement is necessary for any operating temperature and any electrode thickness. The improvement greatly facilitates the accurate pre-evaluation of fuel cell electrodes with a large range of thicknesses and operating temperatures and thus, is of practical importance for the development of highly-efficient fuel cells with high cost-effectiveness and low polarization loss.

Acknowledgments

The authors thank Dr. Kelvin HL Zhang at University of Oxford, Dr. Xiao Lin in Pacific Northwest National Laboratory, and Qian Zhang at Vanderbilt University for their insights.

References

[1] J. Santamaria, J. Garcia-Barriocanal, A. Rivera-Calzada, M. Varela, Z. Sefrioui, E. Iborra, C. Leon, S.J. Pennycook, Science 321 (2008) 676–680.
[2] S. Xu, B.J. Hansen, Z.L. Wang, Nature Communications 1 (2010) 93.
[3] F.R. Fan, Z.Q. Tian, Z.L. Wang, Nano Energy 1 (2012) 328–334.
[4] C. Xu, C. Pan, Y. Liu, Z.L. Wang, Nano Energy 1 (2012) 259–272.
[5] S.S. Mao, B. Liu, X.B. Chen, Y.L. Dong, M.J. Cheng, Advanced Energy Materials 1 (2011) 343–346.
[6] H. Wu, G. Chan, J.W. Choi, I. Ryu, Y. Yao, M.T. McDowell, S.W. Lee, A. Jackson, Y. Yang, L. Hu, Y. Cui, Nature Nanotechnology 7 (2012) 310–315.
[7] H.J. Choi, S.M. Jung, J.M. Seo, D.W. Chang, L. Dai, J.B. Baek, Nano Energy 1 (2012) 534–551.
[8] M. Liu, Y.M. Choi, L. Yang, K. Blinn, W. Qin, P. Liu, M.L. Liu, Nano Energy 1 (2012) 448–455.
[9] M. Zhang, L. Dai, Nano Energy 4 (2012) 514–517.
[10] L.M. Pant, S.K. Mitra, M. Secanell, Journal of Power Sources 206 (2012) 153–160.
[11] Z. Yu, R.N. Carter, Journal of Power Sources 195 (2010) 1079–1084.
[12] C. Chan, N. Zamel, X. Li, J. Shen, Electrochimica Acta 65 (2012) 13–21.
[13] K.J. Yoon, P. Zink, S. Gopalan, U.B. Pal, Journal of Power Sources 172 (2007) 39–49.
[14] J.H. Nam, M. Kaviany, International Journal of Heat and Mass Transfer 46 (2003) 4595–4611.
[15] S.H. Chan, K.A. Khor, Z.T. Xia, Journal of Power Sources 93 (2001) 130–140.
[16] D.L. Sidebottom, Reviews of Modern Physics 81 (2009).
[17] K. Hayamizu, Y. Aihara, S. Arai, C.G. Martinez, Journal of Physical Chemistry B 103 (1999) 519–524.
[18] K.J. Yoon, S. Gopalan, U.B. Pal, Journal of The Electrochemical Society 156 (2009) B311–B317.
[19] K.J. Yoon, S. Gopalan, U.B. Pal, Journal of The Electrochemical Society 154 (2007) B1080–B1087.
[20] W.D. He, K.J. Yoon, R.S. Eriksen, S. Gopalan, S.N. Basu, U.B. Pal, Journal of Power Sources 195 (2010) 532–535.
[21] W.D. He, B. Wang, H. Zhao, Y. Jiao, Journal of Power Sources 196 (2011) 9985–9988.
[22] W.D. He, B. Wang, Advanced Energy Materials 2 (2012) 329–333.
[23] W.D. He, B. Wang, J.H. Dickerson, Nano Energy 1 (2012) 828–832.
[24] E. Fabbri, L. Bi, H. Tanaka, D. Pergolesi, E. Traversa, Advanced Functional Materials 21 (2011) 158–166.
[25] A.J. Jacobson, Chemistry of Materials 22 (2010) 660–674.
[26] E.D. Wachsman, K.T. Lee, Science 334 (2011) 935–939.
[27] Z. Lin, G. Waller, Y. Liu, M. Liu, C.P. Wong, Advanced Energy Materials 2 (2012) 884–888.
[28] T. Howells, E. New, P. Sullivan, T.S. Jones, Advanced Energy Materials 1 (2011) 1085–1088.
[29] J.R. Moore, S. Albert-Seifried, A. Rao, S. Massip, B. Watts, D.J. Morgan, R.H. Friend, C.R. McNeill, H. Sirringhaus, Advanced Energy Materials 1 (2011) 230–240.
[30] H.J. Lee, H. Strathmann, S.H. Moon, Desalination 190 (2006) 43–50.
[31] J. Suffner, S. Kaserer, H. Hahn, C. Roth, F. Ettingshausen, Advanced Energy Materials 1 (2011) 648–654.
[32] B. Tu, W. Li, F. Zhang, Y.Q. Dou, Z.X. Wu, H.J. Liu, X.F. Qian, D. Gu, Y.Y. Xia, D.Y. Zhao, Advanced Energy Materials 1 (2011) 382–386.
[33] J.M. Serra, I. Garcia-Torregrosa, M.P. Lobera, C. Solis, P. Atienzar, Advanced Energy Materials 1 (2011) 618–625.
[34] D. Zhao, J.H. Li, M.K. Song, B.L. Yi, H.M. Zhang, M.L. Liu, Advanced Energy Materials 1 (2011) 203–211.
[35] L. Fan, C. Wang, B. Zhu, Nano Energy 1 (2012) 631–639.
[36] L. Su, Y.X. Gan, Nano Energy 1 (2012) 159–163.